CEBAF PR-91-019
April 1991

CEBAF Beam Instrumentation

R. Rossmanith
Continuous Electron Beam Accelerator Facility
12000 Jefferson Avenue
Newport News, VA 23606

CONTINUOUS
ELECTRON
BEAM
ACCELERATOR
FACILITY

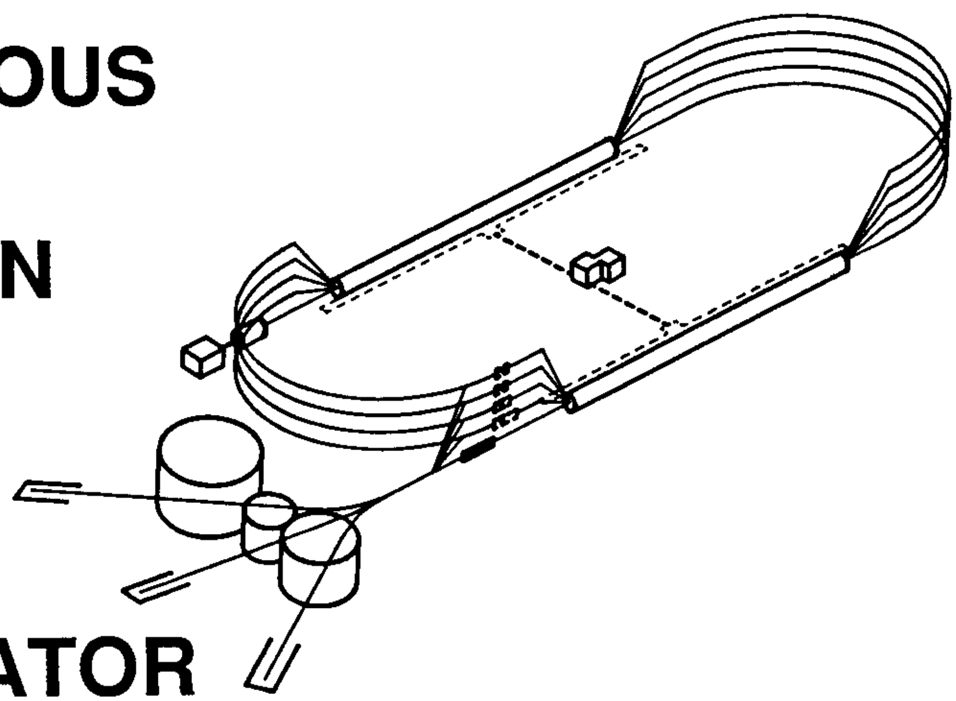

SURA Southeastern Universities Research Association

CEBAF
The Continuous Electron Beam Accelerator Facility
Newport News, Virginia

Copies available from:

Library
CEBAF
12000 Jefferson Avenue
Newport News
Virginia 23606

The Southeastern Universities Research Association (SURA) operates the Continuous Electron Beam Accelerator Facility for the United States Department of Energy under contract DE-AC05-84ER40150.

CEBAF BEAM INSTRUMENTATION*

R. Rossmanith
CEBAF, 12000 Jefferson Ave., Newport News, Virginia 23606, USA

Introduction

CEBAF, now under construction, is a unique accelerator. The main design goals are: (1) a cw electron beam with energies up to 4 GeV; (2) maximum beam current of 200 μA; (3) relative energy spread no larger than 10^{-4}; and (4) support for up to 3 simultaneous fixed target experiments.

The design is indicated in Figure 1. The beam is accelerated in two superconducting linacs. Because the superconducting structure is expensive, about $200 K per meter, the beam is recirculated several times, in a manner somewhat similar to the many passes in a synchrotron. A detailed cost evaluation showed that the lowest total cost could be achieved with five recirculations.

The cavities, which resonate at 1.5 GHz, are similar to the cavities developed at Cornell University. When they were first produced, the maximum achievable gradient was less than 5 MV/m. With experience, the quality has improved so that several cavities have shown gradients significantly larger than 10 MV/meter.

This unconventional machine requires unconventional instrumentation:

- With five beams in the accelerating structures at the same time, the position monitors must be able to detect the position of each beam in the presence of the others.
- Energy spread is closely connected with bunch length, so the bunch length must be measured precisely with sub-picosecond resolution.
- The high power density in the circulating beam makes necessary a system that can shut the machine down within 20 μsec.

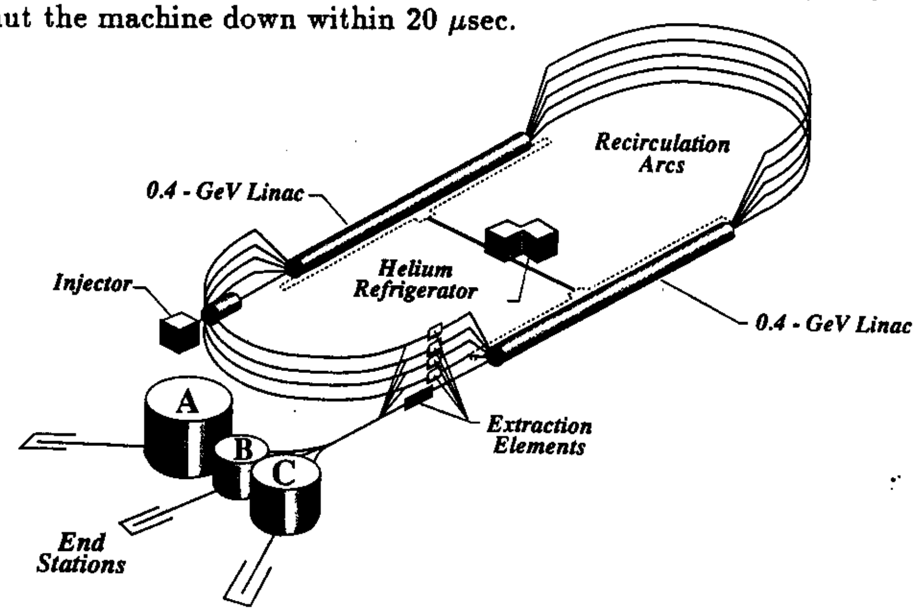

1. The CEBAF accelerator configuration

* This work was supported by the U.S. Department of Energy under contract DE-AC05-84ER40150.

Beam position measurement

As can be seen in Figure 1, all five recirculated beams occupy the same vacuum pipe in the linacs, whereas each beam has its own pipe in the arcs. This implies that different types of monitors must be used in the arcs and the linacs. The linac monitors must be able to measure the position of each beam in the presence of four others; the arc monitors have no such requirement.

Linac monitors. In order to measure the position of each beam individually in the presence of other beams, the beam must be marked, and the mark must then be detected. At CEBAF, the marking is amplitude modulation of the beam current at 100 MHz; the modulation is then further altered by changing its sign, or equivalently shifting its phase by 180°, in a pattern that enables the position monitors to suppress all but the desired signal.[1]

To illustrate the coding for a simple case of two beams, assume

$$f(t) = A\,\sin(\omega t)\,x(t/\tau), \tag{1}$$

where ω is the modulation frequency, τ is the beam circulation period in the machine (4.2 μs for CEBAF), and $x(t/\tau)$ is a function with values ± 1, changing at integer values of its argument. Consider the sequence

$$x = 1, 1, -1, -1, 1, 1-1, -1, \ldots \tag{2}$$

If the signal is mixed with itself, the resulting autocorrelation function is

$$f(t)f(t) = A^2\,\sin^2(\omega t), \tag{3}$$

representing the detected signal for the first pass. The time average is nonvanishing and is equal to $A^2/2$. If $f(t)$ is delayed by τ and then mixed with the detected signal, however, the correlation is

$$f(t)f(t-\tau) = A^2\,\sin^2(\omega t)\,x(t/\tau)\,x(t/\tau - 1). \tag{4}$$

The time average is then

$$\begin{aligned} \frac{1}{T}\int_0^T f(t)f(t-\tau)\,dt &= \frac{A^2}{T}\int_0^T \sin^2(\omega t)\,dt\,(1-1+1-1\ldots) \\ &\approx 0. \end{aligned} \tag{5}$$

Thus, the correlation function in this case picks out the signal from the first pass and suppresses that from the second. To suppress the first and observe the second, the signal is mixed with the delayed sequence $f(t-\tau)$.

The sequence $x(t/\tau)$ is not sufficient for three or more passes, but it is easy to extend the argument. We need only to generate a sequence with values ± 1 such that the autocorrelation function with delay will vanish. Such sequences are already well known in coding theories, where they are known as pseudorandom sequences (PRSs).

To illustrate the technique more carefully, define the correlation function as

$$R(x,y;n) = \frac{1}{T}\int_0^T x(t/\tau)\,y(t/\tau+n)\,dt, \tag{6}$$

where $x(t/\tau)$, $y(t/\tau)$ are pulse sequences with values ± 1, T is the total time of the sequence, and $n\tau$ is the time delay. We are particularly interested in the autocorrelation, $x(t/\tau) = y(t/\tau)$, which should satisfy the orthogonality condition in order for the sequence to act as a filter:

$$\begin{aligned} R(x,x;n) = \frac{1}{T}\int_0^T x(t/\tau)\,x(t/\tau+n)\,dt &= 1 \text{ if } n = 0, \\ &= 0 \text{ if } n \neq 0. \end{aligned} \tag{7}$$

Perfect sequences, which satisfy Eq. 7 exactly, are hard to find and implement. Shift register sequences, however, which will satisfy Eq. 7 to within an arbitrarily small residual error determined by the length of the sequence, can be easily implemented by shift registers with appropriate feedback connections. Programmable array logic (PAL) devices can produce shift register sequences in a single device that needs only a clock pulse. A length-63 PRS generator is indicated in Figure 2; we have used a similar register in our evaluations.

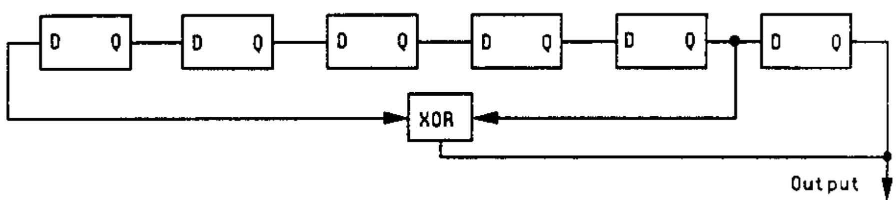

2. Shift register pseudorandom sequence generator (length 63)

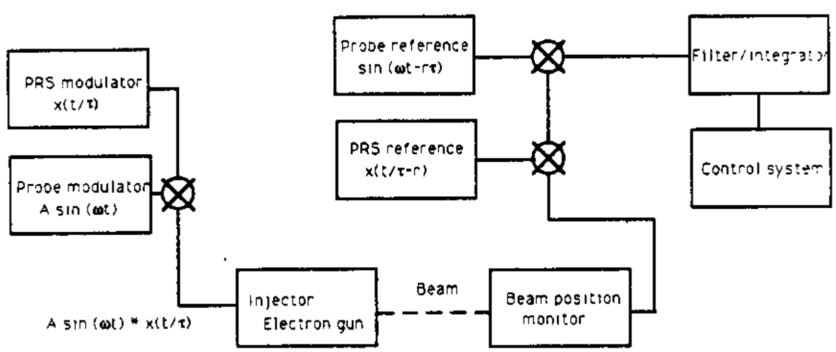

3. Beam position monitor processing

The block diagram for the modulation is shown in Figure 3. The current is modulated with the frequency ω and by a pseudorandom sequence $Ax(t)$,

$$I = I_0 + A\,x(t/\tau)\,\sin(\omega t), \tag{8}$$

where $x(t/\tau)$ is either $+1$ or -1. For five beam passes through the detector, the output signal at the probe is

$$S_d = \sum_{r=0}^{4} \left(k_r A\,x(t/\tau - r)\,\sin(\omega t - r\tau)\right) + \text{noise}, \tag{9}$$

where k_r is a constant for each beam which depends upon its position. Because noise is generally quite system-specific and cannot be easily handled analytically, we will henceforth neglect its effect; as usual, however, noise will determine the processing time needed for a given signal/noise ratio. When the detector signal is mixed with the input delayed by j circulation periods, the output is

$$S = \sum_{r=0}^{4} k_r A^2 x(t/\tau - r)\, x(t/\tau - j)\, \sin^2(\omega t). \tag{10}$$

Integration over m complete sequences will remove the high-frequency time-varying terms, so the signal average will be

$$\overline{S} = \left[\frac{1}{2}k_j A^2 - \frac{1}{2N}\sum_{r\neq j} k_r A^2\right]\left[1 - \frac{\sin 2\omega T}{2\omega T}\right], \tag{11}$$

where ωT is equal to mN; it is seen that the last term in the second brackets is $O(1/T)$.

A position monitor of the type used to observe the beam in the linac regions is the four-wire loop monitor shown in Figure 4.a.

Arc monitors. In the arcs, where each beam has its own beam pipe, the position monitors need not respond to the modulation, so they can be optimized to detect the 1.5 GHz rf signal of the beam. An arc monitor is illustrated in Figure 4.b. The two types of monitors are variations of one basic type, the thin-wire pickup. The general design is shown schematically in Figure 5, where the symbols are defined. The significant differences are found in the termination Z_2, which is ∞ for an open line (1.5 GHz monitor) and 0 for a shorted line (100 MHz monitor).[2,3,4]

For the monitors, the basic quantity of interest is the transfer impedance Z_T, defined for a single pickup as the ratio of the pickup output voltage for a centered beam to the current I_b. The principle of superposition applied to the current sources, plus standard transmission line analysis, gives for the transfer impedance[2]

$$Z_T(\omega) = \frac{g\, Z_1 \parallel Z_c(1 - e^{-j\,2\omega l/c})}{1 - \Gamma_1\Gamma_2 e^{-j\,2\omega l/c}}, \tag{12}$$

where g is a geometric coupling factor, and

$$\begin{aligned} Z_1 \parallel Z_c &= \frac{Z_1\, Z_c}{Z_1 + Z_c} \\ \Gamma_1 &= \frac{Z_1 - Z_c}{Z_1 + Z_c} \\ \Gamma_2 &= \frac{Z_2 - Z_c}{Z_2 + Z_c}. \end{aligned}$$

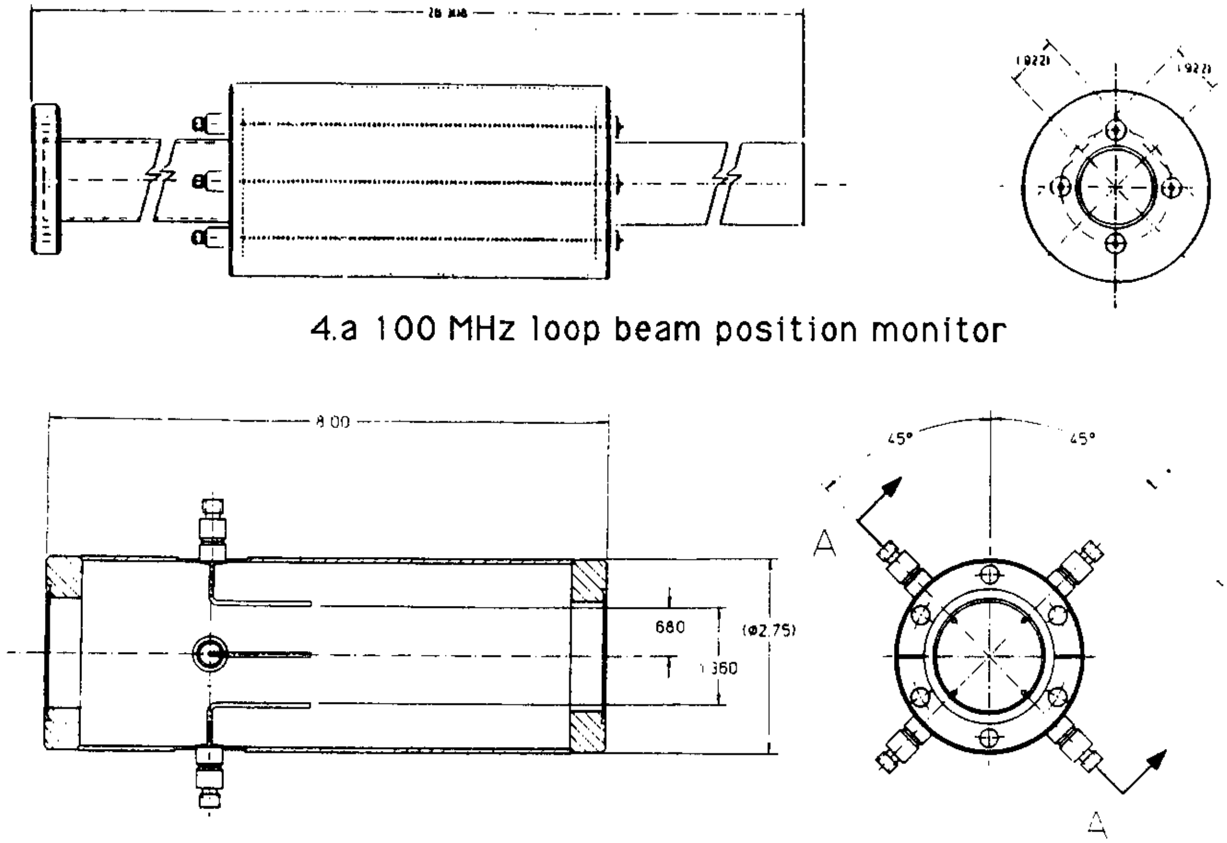

4.a 100 MHz loop beam position monitor

4.b 1500 MHz beam position monitor

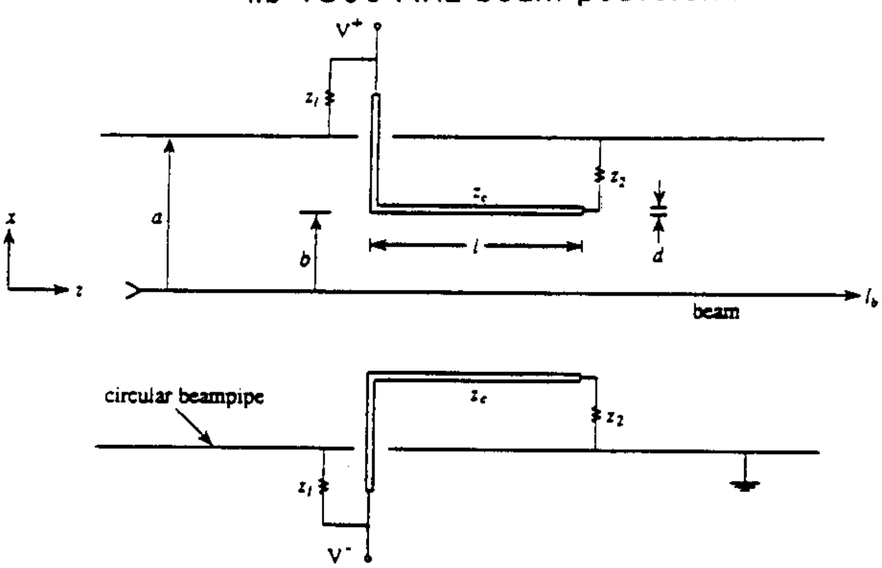

5. General thin-wire beam position monitor

The amplitudes of the transfer impedance for three pickup types are shown in Figure 6. The plots are normalized to gZ_1 and carried out to $4\omega_0$ to emphasize the relative sensitivities and multiple bandpass characteristics of the pickups.

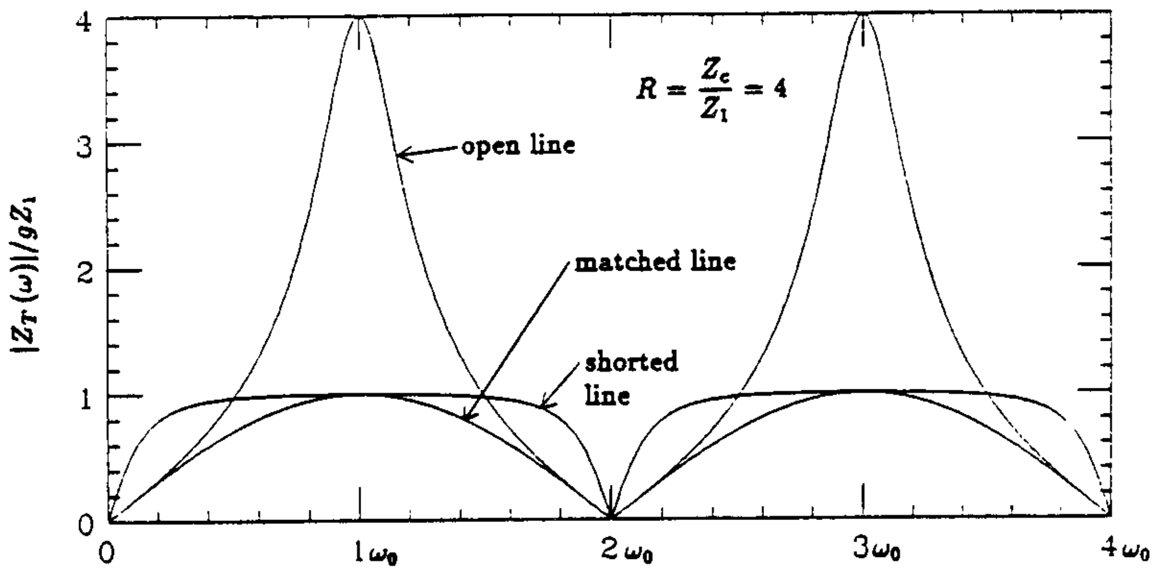

6. Amplitude of transfer impedance vs. frequency

Orbit correction techniques

We have performed orbit corrections,[5] using simulations, for the full five-pass accelerator. The orbit correction of the lowest energy beam is found by making the beam offset in each position monitor zero for the first pass. However, the corrector settings are not necessarily optimum for the higher passes. A perfect orbit correction cannot be obtained simultaneously for all beams.

Since the linac design uses an alternating position monitor and corrector pattern, we can compute the upstream corrector strength required to make a downstream monitor reading zero for the first pass. The necessary kick $\Delta x'_k$ is calculated from the beta functions and phase advance:

$$\Delta x'_k = -\frac{\Delta x_m}{\sqrt{\beta_k \beta_m}\,\sin(\phi_m - \phi_k)\sqrt{p_k/p_m}}. \tag{13}$$

Figure 7 shows the corrected low-energy beam, together with the higher order passes.

Further correction of the higher passes is limited because any change applied to a corrector will disturb the low-energy beam. The following methods can be used for the correction of the higher energies: (1) Optimization of the injection angle and displacement, (2) the use of beam bumps in the low-energy line, which act as kicks for the higher energies, (3) a combination of these, (4) a least-squares fit to 26 variables (26 corrector dipoles with 26 monitor readings), and (5) 36 variables (26 correctors and 10 initial conditions). All of these have been tried in our simulations. As an example of what can be done, Figure 8 shows the results of optimizing the entrance angles and positions of the recirculated beams.

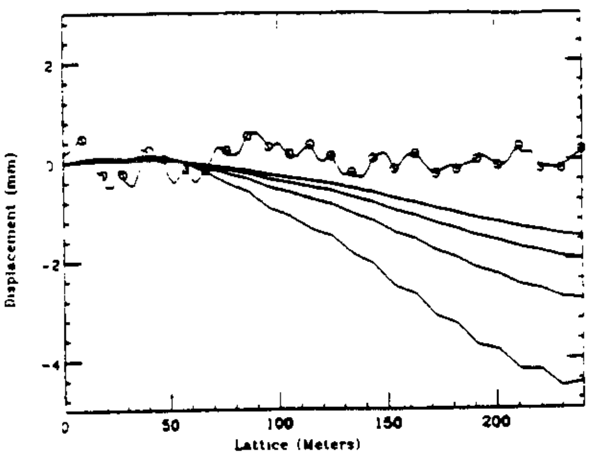

7. Low-energy corrected orbit with higher-energy passes

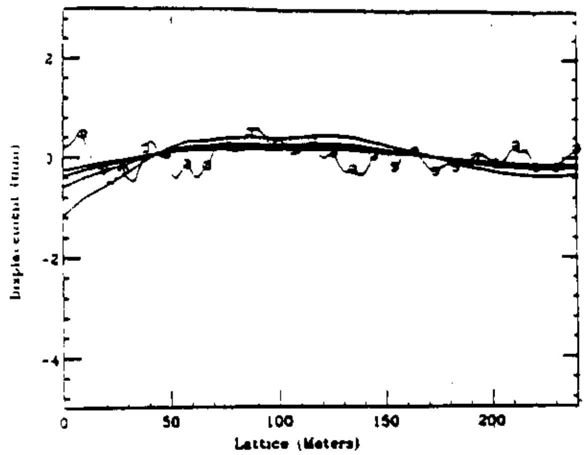

8. Optimization of injection parameters

Bunch length measurement

The bunch length in the CEBAF electron beam, less than 1° in phase or 2 ps in time when fully relativistic, is too short to be measured by direct timing techniques. We have proposed two methods for obtaining subpicosecond resolution:

1. To measure the self-correlation function of the transition radiation emitted when the beam strikes a thin sheet of metal foil; this method is discussed more fully in another paper. (Walter Barry, Proceedings of this conference.)
2. To observe the change in the energy spread that is introduced when the phase between the beam and one or more rf cavities is altered.[6] This method will be described in more detail.

The bunch usually rides at the crest of the rf wave in order to maximize the acceleration and to minimize the energy spread. By altering the phase of one or several cavities, the energy spread can be increased by an amount that is proportional to the bunch length. By measuring the energy spread for several phases, the bunch length can be determined with subpicosecond resolution. The method has been successfully tested at the injector, but can later be used at any part of the accelerator.

The cavities in the injector, shown in Figure 9, are driven by two klystrons. The first cavity raises the beam energy to about 2.7 MeV, which is nearly fully relativistic ($\beta = 0.98$). The phase of the second cavity can then be altered to increase the energy spread. Calculations have indicated that the phase length of the bunch at the entrance of the second cavity can be measured with 0.2° precision; this figure represents the limit of validity of the computation.

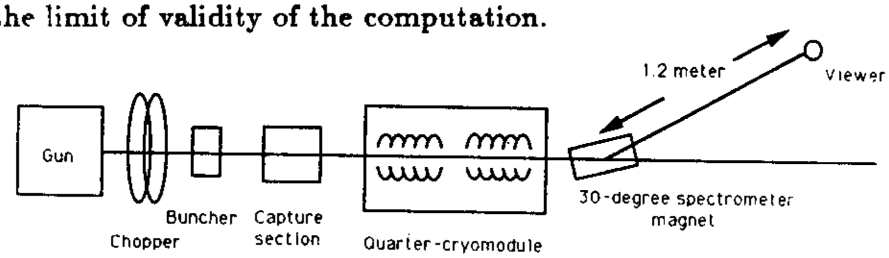

9. Schematic layout of CEBAF injector

To a first approximation, the energy spread produced in the beam by the second rf cavity because of phase spread is given by

$$\delta E = E_0 \sin \phi \, \delta\phi, \tag{14}$$

where E_0 is the energy an electron would gain in traversing the cavity at optimum phase, ϕ is the phase difference of the bunch centroid from optimum, and $\delta\phi$ is the phase spread in the bunch. The bunch length l is related to the phase spread by

$$l = \lambda \beta \, \delta\phi/(2\pi), \tag{15}$$

where λ is the rf wavelength, and $\beta\,(= v/c)$ is very nearly equal to 1. A closer approximation for δE can be gained by using the beam transport code PARMELA, which includes the effects of phase drift that is present because β is not quite equal to 1.

We can characterize the beam by its energy spread δE and its phase spread $\delta\phi$. Their values at the output of a cavity can be connected to their values at the input. Let the subscript i denote input, and o denote output. For small dispersions, we have the following linear relations:

$$\begin{aligned} \delta E_o &= \left(\frac{\partial E_o}{\partial E_i}\right) \delta E_i + \left(\frac{\partial E_o}{\partial \phi_i}\right) \delta\phi_i \\ \delta\phi_o &= \left(\frac{\partial \phi_o}{\partial E_i}\right) \delta E_i + \left(\frac{\partial \phi_o}{\partial \phi_i}\right) \delta\phi_i. \end{aligned} \tag{16}$$

The transfer coefficients $\partial E_o/\partial E_i$, $\partial E_o/\partial \phi_i$ are computed by PARMELA.

The input energy spread δE_i and the input phase spread $\delta\phi_i$ can be found by least squares, yielding as the best fit the following values:

$$\begin{aligned} \delta E_i &= 0.0386 \text{ MeV}, \\ \delta\phi_i &= 0.247^\circ. \end{aligned} \tag{17}$$

Note that, as 1° at 1.5 GHz represents a time of 1.85 ps, the measured bunch length is nearly 450 fs.

Accelerator protection and beam shutdown.

Because of the high power density of the beam, if it is steered into any solid object, it will burn a hole in a very short time, typically of order 0.1 millisecond or less. As a design constraint, it is assumed that the burnthrough time is 50 μs. The beam already launched at the injector can require 25 μs to clear the machine, and another 5 μs may be necessary for transit time to get the shutdown signal to the injector. We thus have approximately 20 μs available for response of the protection system.

To detect beam loss, we have installed a system of counters that detect increases in background radiation.[7] If the background counting rate at any counter increases to more than a preset limit, a signal is sent to the fast shutdown[8] (FSD) system, telling it to turn off the beam at the gun. The turnoff is accomplished in two steps: a large negative voltage is rapidly applied to the grid, and then, somewhat more slowly, the high voltage power is removed from the gun. The shutdown is hardwired separately from the computer controls, although it sends messages to the computer. This means that a computer crash will not disable the FSD system.

The system continually accepts and passes a series of 5 MHz square or trapezoidal waves that must be received to keep the gun active. It is fail-safe in the sense that a power failure emulates an FSD trigger. If the permissive signal does not arrive at any level of the safety logic, that level will initiate shutdown within less than 5 cycles. By comparison, a trigger produced by an actual fault condition will initiate shutdown within 3 cycles, a difference that is equivalent to only one more level of logic.

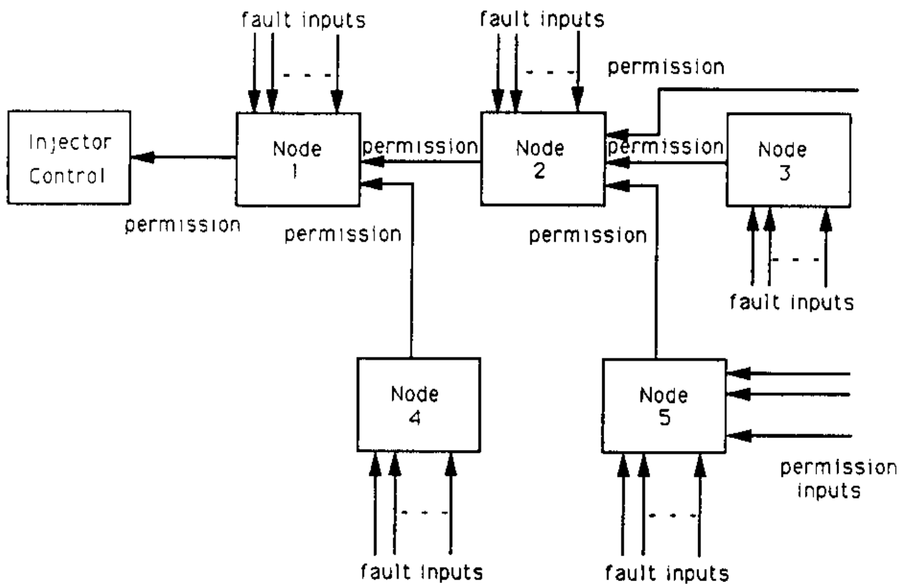

10. Fast shutdown tree structure

While the system was being designed, it became apparent that fault conditions other than beam loss should also shut the beam down. In time, the number of triggers became rather large, so large in fact as to affect the choice of architecture used in implementing the shutdown. To accommodate the large and increasing number of triggers, we have adopted a tree logic (see Figure 10). Up to seven input signals can be received and combined by each node. A positive fault signal on any of the inputs will result in an output fault signal within 3 cycles, or 600 ns. The output signal is then passed on to the next logic level for its action. Since each level introduces its own 600 ns delay, the number of levels cannot be allowed to increase without limit; but the practical limit, corresponding to a total delay of 10 μs, is so large that it does not impose any real constraint.

Viewers and profile monitors

Several conventional diagnostic tools are also installed in the CEBAF beamline. They include about 120 actuators that are distributed around the accelerator, and that can insert or withdraw targets from the beam. The targets can be:

Standard fluorescent screens

Aluminum foils to produce transition radiation

Cherenkov cells.

In addition, we have several profile monitors, wire scanners driven by stepper motors.

The beam current is measured by a Faraday cup at low energy, or it can be monitored on-line by parametric current transformers.

References

1. W. C. Barry, J. W. Heefner, G. S. Jones, J. E. Perry, and R. Rossmanith, "Beam position measurement in the CEBAF recirculating linacs by use of pseudorandom pulse sequences," *Proc 2nd European Particle Accelerator Conf*, 12-16 June 1990, Nice, pp. 723-5. CEBAF-PR-90-009.
2. Walter Barry, "A general analysis of thin wire pickups for high frequency beam position monitors," to be published, *Nucl Inst Methods in Phys Res.* CEBAF-PR-90-024.

   P. Adderley, W. Barry, J. Heefner, P. Kloeppel, and R. Rossmanith, "A beam position monitor for low current dc beams," *Proc 1989 Particle Accelerator Conf*, 20-23 March 1989, Chicago, pp. 1602-4. CEBAF-PR-89-004.
3. W. Barry, R. Rossmanith, and M. Wise, "A simple beam position monitor system for CEBAF," *Proc 1988 Linear Accelerator Conf*, 3-7 October 1988, Newport News, VA, pp. 649-651. CEBAF-PR-89-015.
4. W. Barry, J. Heefner, and J. Perry, "Electronic systems for beam position monitors at CEBAF," *Proc 1990 Instrumentation Workshop*, to be published. CEBAF-PR-90-023.
5. A. Barry, B. Bowling, J. Kewisch, and J. Tang, "Orbit correction techniques for a multipass linac," *Proc 6th Linear Accelerator Conf*, 10-14 Sept 1990, Albuquerque, NM, pp. 444-6. CEBAF-PR-90-016.
6. W. Barry, P. Kloeppel, and R. Rossmanith, "Technique of measuring bunch length by phasing an rf cavity," *Proc 6th Linear Accelerator Conf*, 10-14 Sept 1990, Albuquerque, NM, pp. 719-720. CEBAF-PR-90-014.
7. John Perry, "The beam loss monitors at CEBAF," *Proc 1990 Instrumentation Workshop*, to be published. CEBAF-PR-90-022.
8. J. Perry and E. Woodworth, "The CEBAF fast shutdown system," *Proc 6th Linear Accelerator Conf*, 10-14 Sept 1990, Albuquerque, NM, pp. 484-6. CEBAF-PR-90-015.